

Stress State of Uzbekistan's Seismically Active Areas

Yu. L. Rebetsky^{a, *}, T. L. Ibragimova^b, R. S. Ibragimov^b, and M. A. Mirzaev^b

^a*Schmidt Institute of Physics of the Earth, Russian Academy of Sciences, Moscow, Russia*

^b*Mavlyanov Institute of Seismology, Academy of Sciences of the Republic of Uzbekistan, Tashkent, Uzbekistan*

*e-mail: reb@ifz.ru

Abstract—The current stress state of the Earth's crust in the territory of Uzbekistan was studied by cataclastic analysis of displacements along fault sets for the collected catalog of earthquake focal mechanisms (EFM), compiled from the data of different authors. Two stages of stress field reconstruction are implemented at different levels of area detail of averaging parameters and for different magnitude hierarchies of the analyzed earthquakes. Azimuths and dip angles of principal stresses axes, Lode–Nadai coefficient values, geodynamic type of stress state, relative (normalized to the cohesion strength of the rock massif) normalized values of the maximum shear stress and effective pressure are determined for different areas of the studied territory. As a result of natural stress reconstructions based on the focal mechanisms of earthquakes with magnitudes $M \leq 4.5$ and $M \geq 5$, differences in the parameters of the stressed state were revealed. It has been suggested that the hierarchy of magnitude levels of the considered earthquakes reflects the stressed state of various deep layers of the crust. It is shown that strong earthquakes gravitate to zones of reduced effective pressure. On this basis, segments of active faults have been identified in the territory of eastern Uzbekistan, which are considered zones of potentially increased seismic hazard.

Keywords: earthquake focal mechanism, stress field reconstruction, principal stress axes, stress ellipsoid, geodynamic type of stress state

DOI: 10.3103/S0747923920060079

INTRODUCTION

The territory of Uzbekistan is characterized by a complex tectonic structure and a high level of seismic activity. Its eastern part belongs to the neotectonic epiplatform orogen of the Western Tien Shan; the western part, to the epi-Hercynian Turan platform. In the territory of Uzbekistan and adjacent regions, both during the historical period and at present, earthquakes with magnitudes of $M \geq 7$ and epicentral shock intensities of $I_0 = 9–10$ on the MSK-64 scale have repeatedly occurred. Therefore, the problem of ensuring seismic safety is very relevant here.

The solution of a number of important applied seismology problems related to earthquake prediction and hazard assessment of seismically active regions relies heavily on the results of studies of the modern stress-strain state of crustal structures due to ongoing geodynamic processes. Various aspects of the global problem of assessing the stress-strain state of seismically active structures in the study area are discussed in a number of papers (Shirokova, 1974; Gzovsky, 1975; Gushchenko, Sim, 1977; Gushchenko et al., 1977; Riznichenko et al., 1982; Cabin boy, 1990; Nikolaev 1992; Kuznetsova et al., 1995; Ibragimov et al., 2002; Trifonov et al., 2002; Hamidov, 2004; Umurzakov, 2010; Atabekov, 2020, etc.), which were carried out at different times based on analysis of seismological and

geological stress indicators, as well as mathematical modeling of tectonic processes.

Data on earthquake focal mechanisms provided important information about the stresses removed at the time of the earthquake and the fault kinematics. In quantitative seismic hazard assessments, this information is widely used in selecting the proper ground motion prediction equation (GMPE), since the level of seismic impacts depends on the kinematic type of slip at the source (<http://www.gmpe.org.uk/>, etc.).

Temporal fluctuations in the azimuths and dip angles of the axes of tensile and compressive stresses at the sources of weak and moderate earthquakes may indicate changes in the stress state of rock massifs associated with preparation of a strong earthquake; hence, they are used in earthquake prediction (Sobolev and Ponomarev, 2003; etc.). To date, various methods have been developed for reconstructing the stress-strain state of the crust, based on interpretation of the set of earthquake focal mechanisms that characterize quasiuniformly deforming volumes of the crust (Riznichenko 1985; Yunga, 1990; Gushchenko, 1996; Rebetsky 1997; etc.). The features of the stress state of seismically active structures revealed from the results of reconstructions, combined with information on the dip angles of faults and values of the stresses released at the sources of moderate earthquakes, can be useful

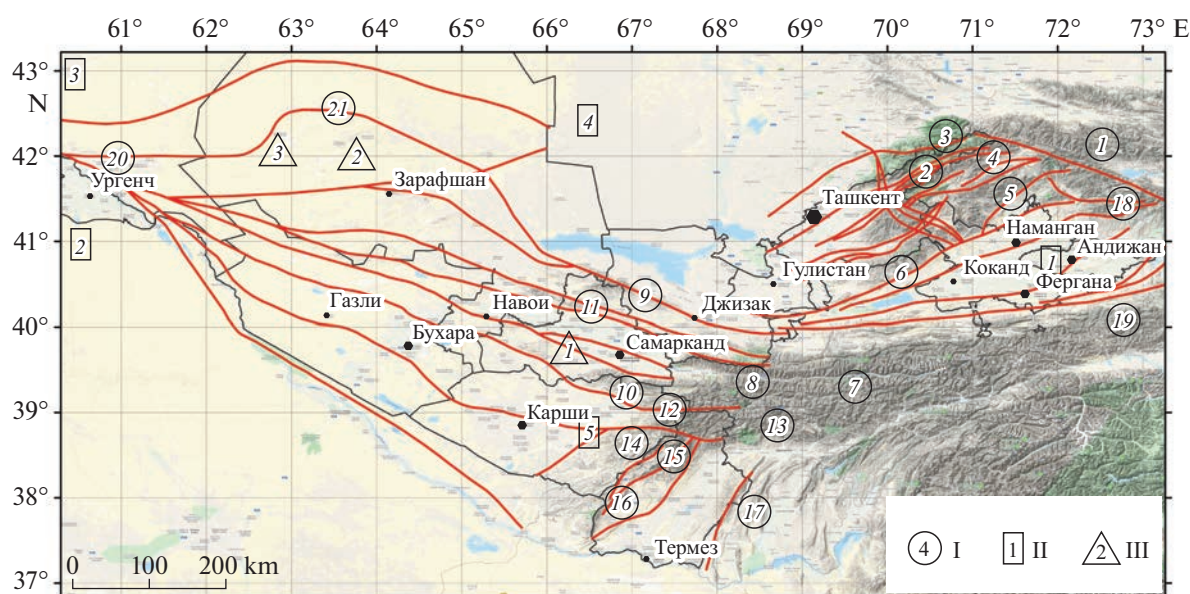


Fig. 1. Modern structural map of study area and active crustal faults (after (Ibragimov et al., 2002)). I, Ridges: 1, Talas; 2, Ugamsky; 3, Karzhantau; 4, Pskemsky; 5, Chatkalsky; 6, Kuraminsky; 7, Turkestan; 8, Malguzar; 9, Nuratinsky; 10, Zirabulak-Ziaetdinsky; eleven, Zerafshansky; 12, Gabryntau; 13, Gissar; fourteen, Baysuntau; 15, Surkhantau; sixteen, Kugitantau; 17, Babatag; 18, Fergana nineteen, Alai; 20, Sultanuizdag; 21, Bukantau. II, troughs: 1, Fergana 2, Amu Darya; 3, Aral; 4, Syrdarya; 5, Kashkadarya; 6, Ayakagytma. III, deflections: 1, Zerafshansky; 2, Jamikum; 3, Mingbulaksky. Lines, active faults.

for identifying fault segments most favorable for large-scale faulting (Rebetsky and Kuzikov, 2016).

Despite the wide range of problems solved with earthquake focal mechanisms, a small number of which have been mentioned above, in many countries of the post-Soviet space, mass determinations of mechanisms, unfortunately, have not been carried out for a long time. This fully applies to the territory of Uzbekistan, where the mass determination of mechanisms of earthquakes with a magnitude $M \geq 3.5$ have only recently resumed after almost 30 years. Therefore, the data accumulated earlier in various sources on the determinations of the earthquake focal mechanisms in the study area are very valuable.

The article analyzes the combined catalog of earthquake focal mechanisms (EFM) of the territory of Uzbekistan, compiled from data from different authors. Using the combined catalog of EFM, inversion of natural stresses was carried out by the cataclastic analysis method of discontinuous displacements (CAM) (Rebetsky 1997). The natural stresses were reconstructed at various levels of area detail and magnitude hierarchy of the considered earthquakes.

BRIEF DESCRIPTION OF THE STUDY AREA

The study area is located in the central part of the Western Tien Shan between the Central Kazakhstan shield and the Turan Plate of the Ural–Siberian platform in the north and west, the Tarim block in the east, and the Indian Platform in the south (Ulomov,

1974). The eastern part of the study area includes the Tien Shan, Alai, and Pamir mountain systems. The Kopetdag Range of the Turkmen–Khorasan mountain system is located to the southwest of Uzbekistan.

The geological structures of the Western Tien Shan (Fig. 1) differ significantly in relief, geological structure, and history of geological development. In the east, they are represented by high mountain folded structures, consisting of Paleozoic formations, and intermontane and piedmont basins, covered by Mesozoic and Cenozoic sediments. In the west, these sediments, smaller in thickness, overlie the vast plains of the Epipaleozoic Turan Plate; Paleozoic rocks sometimes appear as small elevations within the Kyzylkum.

Within the Turan Plate, the Amu Darya, Syr Darya, and Aral basins are distinguished. The epiplat-form orogenic region includes a system of positive and negative structures expressed in the relief as mountain ranges (Chatkalo-Kurama, Alai-Turkestan, Zerafshansky-Gissar, etc.), intermontane (Fergana, Surkhandarya) and piedmont (Tashkent-Golodnostepa, Kashkadarya) basins and discontinuous fault zones separating them. In this study, we used the seismotectonic basis proposed in (Ibragimov et al., 2002).

According to geological and geophysical data within the study area, the thickness of the crust varies from 40 km in the northwest (Aral Sea region) to 55 km (Fergana Valley).

Figure 2 shows a map of the earthquake epicenters of the studied region, constructed from the catalog compiled at the Mavlyanov Institute of Seismology,

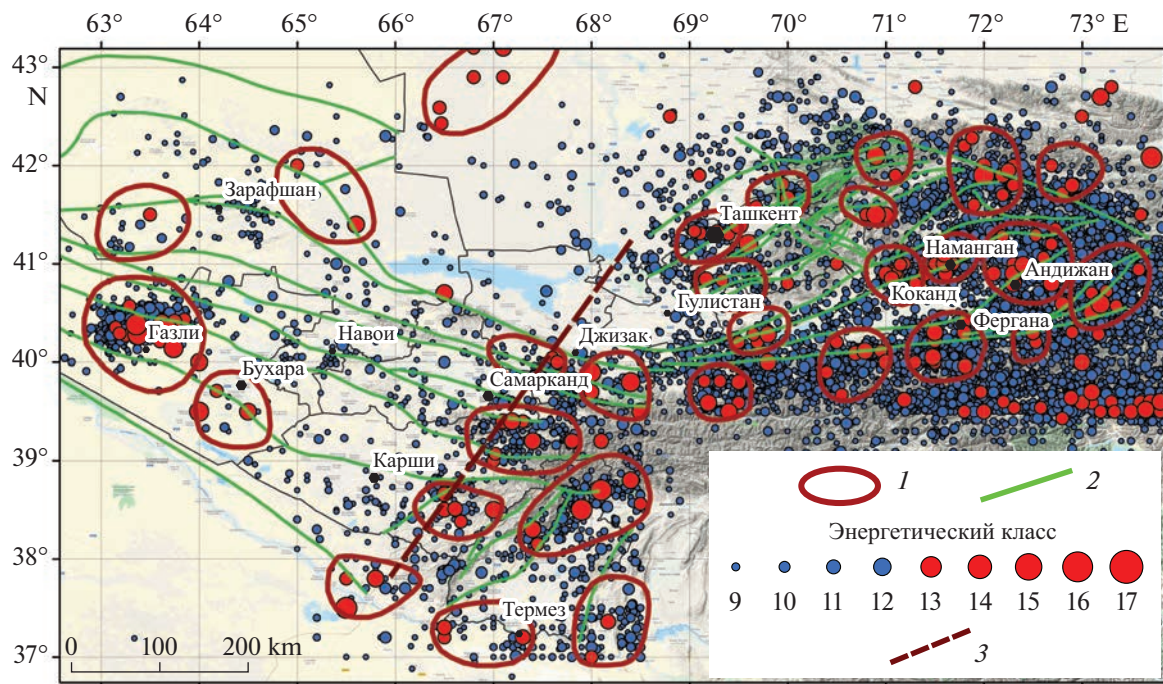


Fig. 2. Map of epicenters of historical and instrumental earthquakes with energy class $K = 9-17$ ($M = 2.5-7.5$) in the study area indicating active crustal faults and areas with high concentration of strong earthquakes: (1) focal zones; (2) active faults; (3) West Tien Shan lineament. Circles, earthquake epicenters.

Academy of Sciences of the Republic of Uzbekistan. The catalog includes parameters of historical and instrumental earthquakes. In the regional catalog, the energy class K of earthquakes is the main characteristic for classifying them by magnitude, determined by the sum of the amplitudes of P - and S -waves recorded by short-period equipment (Rautian 1960; Rautian et al., 2007). The energy class is related to the seismic energy E released during earthquakes as the dependence $K = \log E(J)$. Transition from energy class K to local (Richter) magnitude M_L (hereinafter simply M) and moment magnitude M_W used in the CMT-catalog of EFM was carried out based on the dependences of (Mukambaev and Mikhailova, 2014) for the territory of Central Asia.

The distribution of epicenters of strong earthquakes over the area (see Fig. 2) is very uneven. East of the West Tien Shan lineament, which is the boundary between the Tien Shan mountains and the plain territory of the Turan Plate, seismic activity both at the level of weak and moderate seismic events and at the level of strong earthquakes is very high; west of this line, it is low (Artikov et al., 2020). The increased density of epicenters of strong earthquakes in western Uzbekistan are characterized by the areas of Gazli and Bukhara. Several strong earthquakes were noted in the area of the Central Kyzylkum.

The vast majority of strong earthquakes in the study region occur in fairly narrow, extended zones associated with deep crustal faults. Within seismically

active zones, areas have been distinguished in which seismic activity at the level of strong earthquakes recorded since historical times was very high. Comparison of the maps of earthquake epicenters constructed over different time intervals (until 1900 and beginning with the instrumental period) shows that the identified areas with high concentrations of strong earthquakes maintain their configuration quite stably, which indicates the presence of favorable conditions for large-scale faulting in the field of acting tectonic stresses. Due to the low variability of seismotectonic processes determining the current stress state seismically active structures over tens and hundreds of years, these intense crustal crush zones are considered as the most likely areas of expected seismic activation in the coming decades (Artikov et al., 2017; Artikov et al., 2018). A tectonophysical description of these areas is of considerable interest.

EFM CATALOG

In forming the EFM database, in addition to constructions published in the digests *Earthquakes in Central Asia and Kazakhstan (Zemlyatryaseniya..., 1979-1988)*, the following sources were used:

focal mechanisms of strong (with $M \geq 5$) earthquakes that occurred on the territory of Uzbekistan and adjacent territories from 1946 to 1985 determined by E.M. Bezrodnyi and explained in (Bezrodnyi and Tuichiev, 1987) (41 constructions); a sampling of

earthquakes over the territory of Uzbekistan from the EFM catalog for Central Asia with energy class $K \geq 10$ ($M \geq 3.5$) for the period from 1970 to 2005 (N.N. Mikhailova and N.N. Poleshko, authors), presented by Deputy Science Director of IGR ME RK N.N. Mikhailova (539 constructions); a sampling of focal mechanisms of earthquakes with magnitude $M \geq 3$ in the territory bounded by coordinates $37^\circ\text{--}43^\circ\text{ N}$, $63^\circ\text{--}74^\circ\text{ E}$ for the period from 1946 to 1992 from the IPE RAS catalog.

There are 326 constructed mechanisms directly related to the study area in this sampling; other events of the sampling were attributed to the neighboring territories of Kyrgyzstan and Tajikistan. For a number of earthquakes, this catalog contains several solutions obtained by different authors:

the Harvard Global Centroid Moment Tensor Catalog (CMT) for earthquakes with $M \geq 5$, (Eksrom and Nettles, 2014) from 1976 to the present (61 determinations).

It should be noted that in the data given in the digests *Earthquakes in Central Asia and Kazakhstan*, in the catalogs of E.M. Bezrodnyi and N.N. Mikhailova, and for most of the events from the IPE RAS catalog, the EFM parameters were determined from the signs of the first arrivals of P -waves, while the solutions in the CMT catalog are based on waveform analysis. The information in each of the databases is not the same. In some sources, the dip angle of the axes of compression and tension is measured from the horizon; in others, from the vertical. Thus, the EFM material we collected for Uzbekistan was extremely heterogeneous.

The primary tasks in forming a consolidated EFM catalog for the territory of Uzbekistan were to bring the initial data to a homogeneous form and choose from the set of different solutions only the most probable for the same seismic events. As a first approximation, Rebetsky (2020) assesses the reliability of the construction of mechanisms in the catalogs of different authors and considers the closeness of their EFM constructions to the solutions in the CMT catalog. Table 1 compares the solutions of different authors for some common seismic events in both the CMT and catalogs of Bezrodnyi and Mikhailova and IPE RAS. As follows from the data in the table, for most seismic events, Bezrodnyi's constructions are close to those of the Harvard CMT catalog.

A significant number of events common to the CMT and Mikhailova's catalogs since 1987 have different EFM solutions. For a number of seismic events, the constructions of different authors are given in the IPE RAS catalog: A. Mostryukova (MOS), S.L. Yunga (YNG), A. Dzevonsky (DZE), and Sipkin (SIP); constructions borrowed from the catalog of the Moscow International Data Center (MCD); solutions published in the yearbook *Earthquakes in the USSR* (CCC).

Based on analysis of the above sources, a single EFM catalog for the territory of Uzbekistan was formed, which includes 1157 seismic events. Figure 3a shows a map of earthquake epicenters included in the consolidated catalog with a depiction of their focal mechanisms. Figures 3b and 3c show histograms of the earthquake distribution from the EFM catalog for Uzbekistan in terms of magnitude and depth.

Figure 4 presents compass diagrams of the spatial distribution of azimuths and dip angles of the axes of tensile and compressive stresses removed at the time of the earthquake for the entire studied region and for individual areas.

As can be seen from Figs. 3 and 4, for the entire territory of Uzbekistan, the submeridional direction of the axis of compression and sublatitudinal direction of the axis of tension predominate. The azimuth of the axis of tension has a slightly larger spread than the axis of compression. Analysis of the dip angles of the axes of compression and tension indicates that for most seismic events, the first is subhorizontal, and the second, subvertical. Thus, the nature of the spatial distribution of the axes of compression and tension in the sources of weak and moderate earthquakes (namely, the vast majority of such events in the consolidated catalog) for the entire study area agrees well with the same characteristics of focal mechanisms of strong earthquakes determined previously (Bezrodnyi and Tuichiev, 1987). At the same time, the distribution of the same parameters for individual regions (see Fig. 4) demonstrates significant variability.

Figure 5 shows the area distribution of earthquakes from the consolidated EFM catalog for six kinematic types of faulting at the source in accordance with the classification proposed in (Rebetsky, 1997). In the study area, all types of focal mechanisms are found, but reverse and transpressional faults predominate. The subhorizontal position of the axis of compression P and subvertical position of the axis of tension T corresponds to these types of focal mechanisms. A significant number of normal and transtensional faults in the eastern part of the territory occurred within the narrow Alai Valley between the South Fergana and South Tien Shan faults, in the central part of the Talas-Fergana fault, and within the Fergana intermontane basin.

On the platform part of the study area, normal faults have been noted in the northwest within the Syrdarya basin, where in 1968 a large-magnitude swarm of Kyzylkum earthquakes occurred. A significant number of normal and transtensional faults can be seen in the Gazli focal zone. This type of mechanism corresponds to the subhorizontal position of the axis of tension T and subvertical position of the axis of compression P . Shear-type earthquakes, which are characterized by a subhorizontal position of the axes of compression and tension, are very rare. The same applies to downcutting (slip) mechanisms.

Table 1. Comparison of constructions of focal mechanisms of some strong earthquakes according to catalogs of E.M. Bezrodnyi, N.N. Mikhailova, and IPE RAS with solutions of mechanisms in CMT catalog



























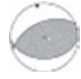






































No.	Date	M_w	H , km	CMT data	E.M. Bezrodnyi's data	N.N. Mikhailova's data	IPE RAS catalog	
							source	mechanism
1	08.04.1976	6.6	15				MOS	
2	17.05.1976	6.7	15				MOS	
3	31.01.1977	6.0	10				CCC	
4	03.06.1977	5.3	24			—	—	—
5	04.06.1978	5.6	10				MOS	
6	06.05.1982	5.7	15				MCD	
							CCC	
7	15.02.1984	5.2	15				YNG	
							MCD	
8	17.02.1984	5.5	12				YNG	
							CCC	
							YNG	
9	23.02.1984	5.2	15		—	—	DZE	
							MCD	
							CCC	

Table 1. (Contd.)

No.	Date	M_w	H , km	CMT data	E.M. Bezrodnyi's data	N.N. Mikhailova's data	IPE RAS catalog	
							source	mechanism
							YNG	
							SIP	
							DZE	
10	19.03.1984	7.0	15				MCD	
							MCD	
							MCD	
							CCC	
							YNG	
							MCD	
11	13.10.1985	5.8	10		–		MCD	
							CCC	
							CCC	
							YNG	
12	26.03.1987	5.2	15		–		CCC	
13	06.11.1992	5.0	19		–		–	–
14	20.02.1995	5.1	33		–		–	–
15	08.10.1995	5.7	20		–		–	–

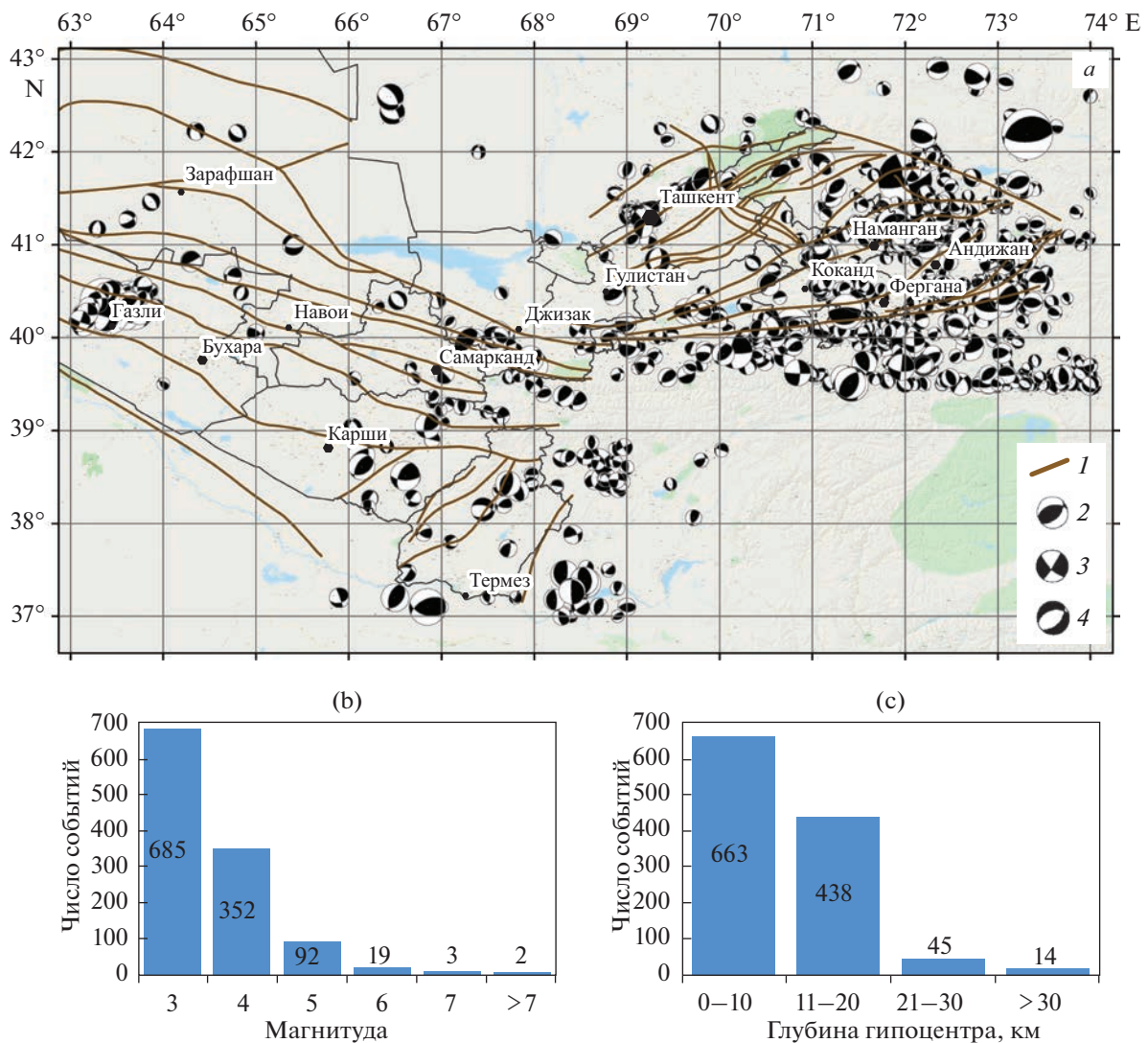


Fig. 3. Map of earthquake focal mechanisms (a) included in consolidated EFM catalog in territory of Uzbekistan and histograms of their magnitude (b) and depth (c) distributions. (1) Active faults; (2) reverse faults; (3) strike-slip; (4) normal faults.

The natural stresses based on EFM data were reconstructed using CAM algorithms developed at the Laboratory of Fundamental and Applied Problems of Tectonophysics, IPE RAS (Rebetsky, 1997). The parameters characterizing the stress state of rock massifs were calculated at various levels of detail. Initially, in order to obtain the generalized pattern of the stress state of the studied region, calculations were performed on a $0.2^\circ \times 0.2^\circ$ grid with a minimum uniform sampling size of 5 EFM determinations in each domain. In this case, the radius of the circular domain within which the necessary number of events were selected for uniform samplings at each calculation point varied from 15 to 60 km.

The reconstruction carried out at this level of detail made it possible to obtain parameters of the stress state of virtually the entire seismically active part of the territory of Uzbekistan (Fig. 6). The exception was a few

areas in which, even with such mild restrictions for statistical reasons, the reconstruction could not be carried out. In the Pritashkent region, this is an area controlled by the dynamic influence of the NE-trending North Angren and South Angren faults, located southeast of Tashkent, within which several strong earthquakes have occurred over the past decades with $M \geq 5$ (Koshtepinskoe 1965; Bukinskoe 1968; Pskent 1970; Tuyabuguz 2013). In the territory of western Uzbekistan, these are two regions: the first is the junction zone of the NW-trending Besapan faults system with the NE-trending North Tamdinsky fault system (northeast of Zharafshan), where in 1969 a swarm of Kyzylkum earthquakes with $M \geq 5$ occurred; the second is the area of Bukhara, where strong earthquakes have been known since historical times and the last seismic activation at the level of earthquakes with $M \geq 5$ occurred in 2005. On the territory of southern

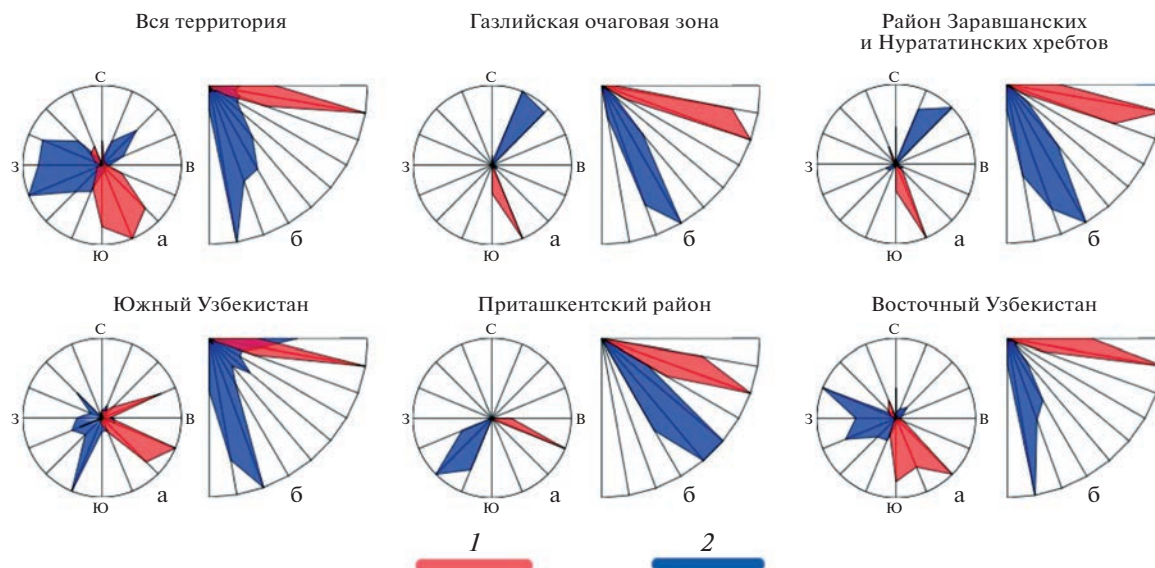


Fig. 4. Compass diagrams of representative azimuths and dip angles of axes of compression (*P*) and tension (*T*) at earthquakes source for territory of Uzbekistan. (*1*) axis of compression; (*2*) axis of tension.

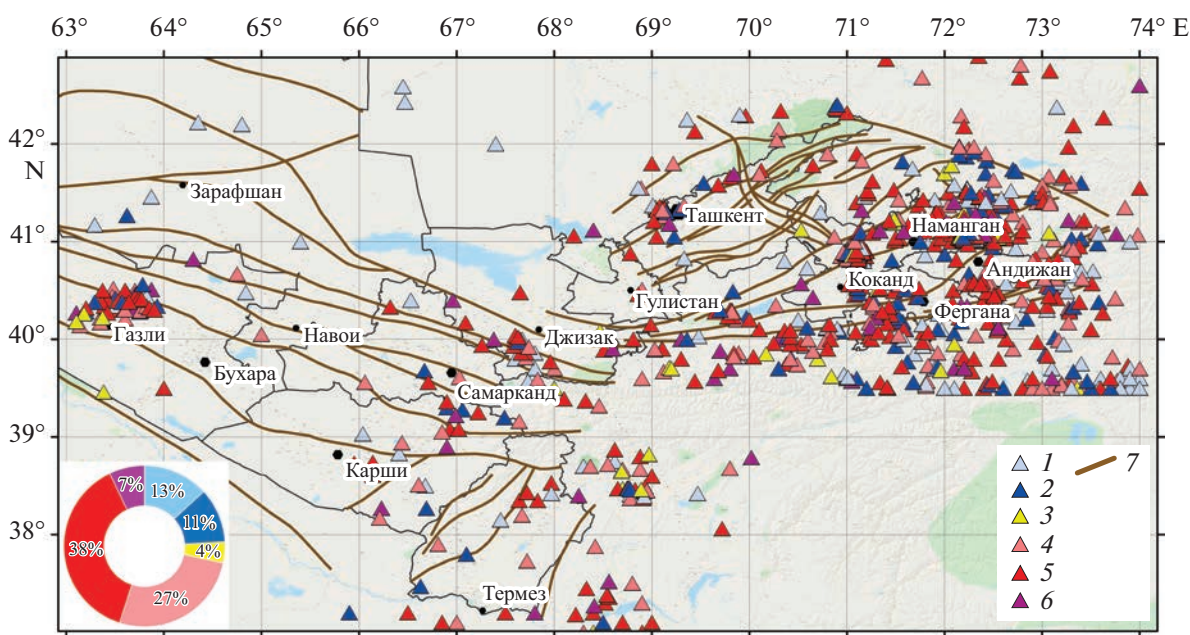


Fig. 5. Area distribution of earthquakes with different kinematic types of rupture in source (after (Rebetsky 1997)). 1–6, kinematic types of ruptures in source: (1) normal fault; (2) transtensional; (3) strike-slip along strike; (4) transpressional; (5) reverse fault; (6) downcut or gentle slope; (7) active faults.

Uzbekistan, these are the areas of the SW-trending Kyzyl-Darya-Langarsky and Baysun-Kugitan faults. Within the first of them, the most famous are the 1971 Langar earthquake with magnitude $M = 5.5$ and a swarm of Kamashinsky earthquakes in 1999–2001, the

largest with a magnitude $M = 5.6$; within the second, Baysun earthquakes of 1935 and 1968, which also had magnitudes of $M \geq 5$.

At the next stage of the study, in order to obtain a more detailed picture of the distribution of natural

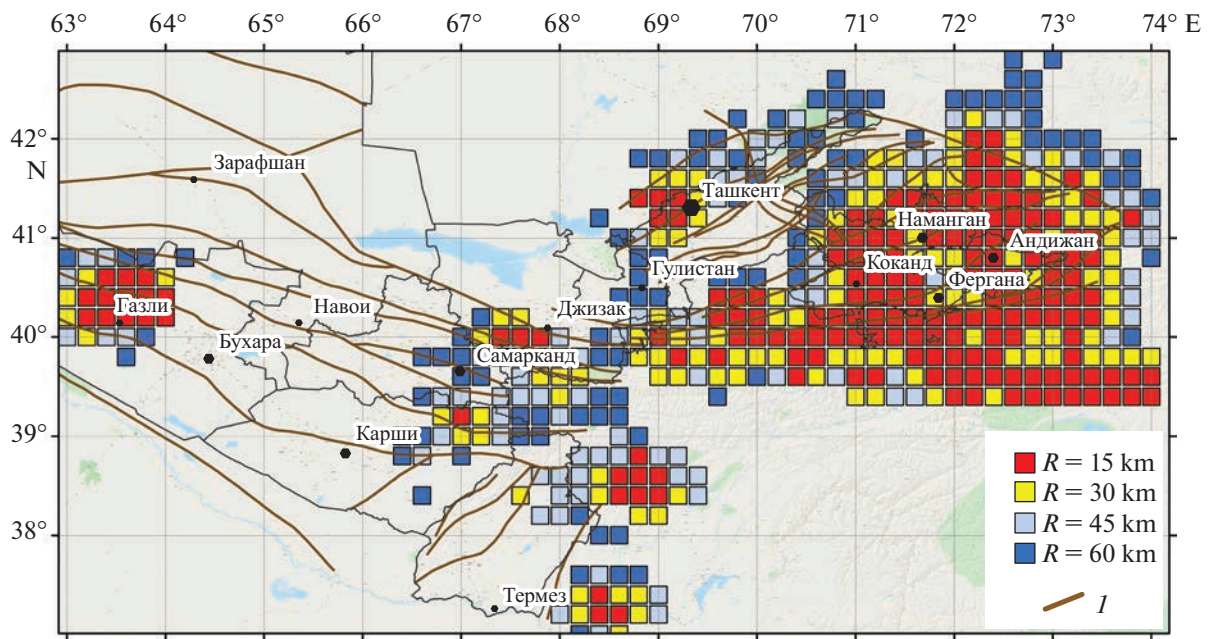


Fig. 6. Zoning of study area according to stress averaging scale. Sectors for which selection of minimum size of a uniform sampling containing at least 5 events ($N \geq 5$) were provided from circular regions with different radii ($15 \leq R \leq 60$ km). *I*, active faults.

stresses in the study area, calculations were performed on a $0.1^\circ \times 0.1^\circ$ grid. The minimum size of a uniform sampling in each studied domain in this calculation variant included at least six definitions of mechanisms; the radius of the circular domain within which the parameters were averaged varied significantly less than before, ranging from 15 to 30 km. This, on the one hand, slightly reduced the area on which reconstruction was possible, and on the other hand, ensured high accuracy of construction in areas where reconstruction was possible. The reconstruction was carried out separately according to the focal mechanisms of weak and moderate earthquakes with $M \leq 4.5$ and for strong earthquakes with $M \geq 5$. Figures 7 and 8 show the domains for which it was possible to reconstruct natural stresses under more stringent restrictions in the mentioned magnitude ranges.

At the selected levels of area detail and magnitude hierarchy of the considered earthquakes, CAM algorithms were employed to obtain a two-stage reconstruction of the field of natural stresses, which made it possible to determine the azimuths and dip angles of the axes of principal stresses, the Lode–Nadai coefficients, geodynamic type of stress state, and relative (normalized to the cohesion strength of rock massifs) values of maximum tangential stresses and effective uniform pressure on the brittle fracture plane.

Prior to their analysis, it should be noted that in the CAM algorithm, the stress sign rule adopted in classical mechanics is used; i.e., compressive stresses are considered negative and tensile stresses positive. Due to this, the principal stresses σ_1 are minimal compressive,

and σ_3 , maximum compressive. In interpreting the orientation of the axes of principal stresses for σ_1 , we use the term “principal tension” (bearing in mind the deviatoric component of this stress), and for σ_3 , principal compression.

STRESS RECONSTRUCTION RESULTS

Voltage Ellipsoid Parameters

Figures 9–10 show the projections onto the horizontal plane of the axes of principal compressive (σ_3) and tensile (σ_1) stresses in each domain for various versions of the reconstruction. Figures 9a and 10a also show the main seismogenic zones of the territory of Uzbekistan (Ibragimov et al., 2002). As follows from Fig. 10a, the dip angle of the axis of minimum compression σ_1 varies greatly for different parts of the study area, varying from vertical in southern Uzbekistan and in individual sections of the Besapan and South Fergana faults to almost horizontal in the Alai Valley beyond the ridge of the same name.

Variations in the dip angle of the axis of principal compressive stress σ_3 within the study area is significantly less (see Fig. 9a). For most of the territory, this axis is subhorizontal. In most cases, the strike of the axis of maximum compression is almost perpendicular to the strike of the structures. This feature is violated for the southeastern part of the Talas–Fergana fault, where the directions of the σ_3 axis and the fault almost coincide. On the territory of the Turan Platform (western Uzbekistan) and within the orogen–platform transition zone (Pritashkent region), the predominant

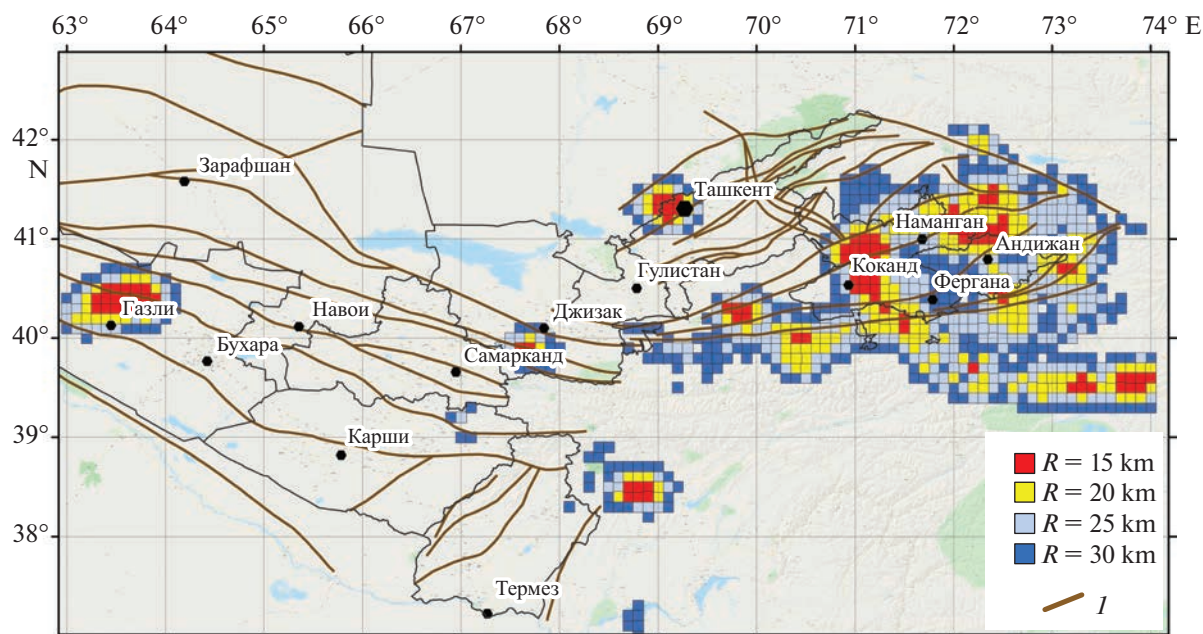


Fig. 7. Domain for which it was possible to reconstruct stresses based on focal mechanisms of earthquakes with $M \leq 4.5$ from consolidated EFM catalog with minimum size of uniform sampling $N \geq 6$ and radius $R \leq 30$ km of circular domain from which required number of events for single domain were selected. (I) Active faults.

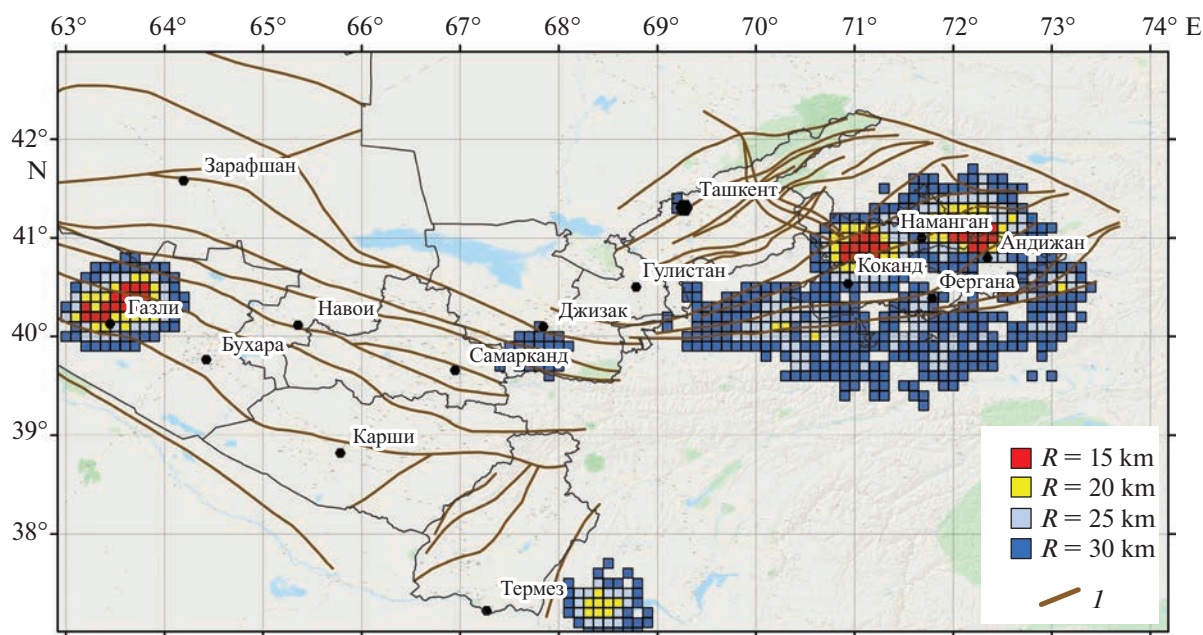


Fig. 8. Domain for which it was possible to reconstruct stresses based on focal mechanisms of earthquakes with $M \geq 5$ from consolidated EFM catalog with minimum uniform sampling size $N \geq 6$ and radius $R \leq 30$ km of circular domain from which required number of events for single domain were selected. (I) Active faults.

direction of the axis of maximum compression σ_3 is southeastern, and in the orogenic part of the study area (eastern Uzbekistan), submeridional.

At the detailed level of the reconstruction (see Figs. 9b, 9c, 10b, 10c), in a number of domains, some differences in azimuths and dip angles of the axes of principal stresses σ_3 and σ_1 are observed when

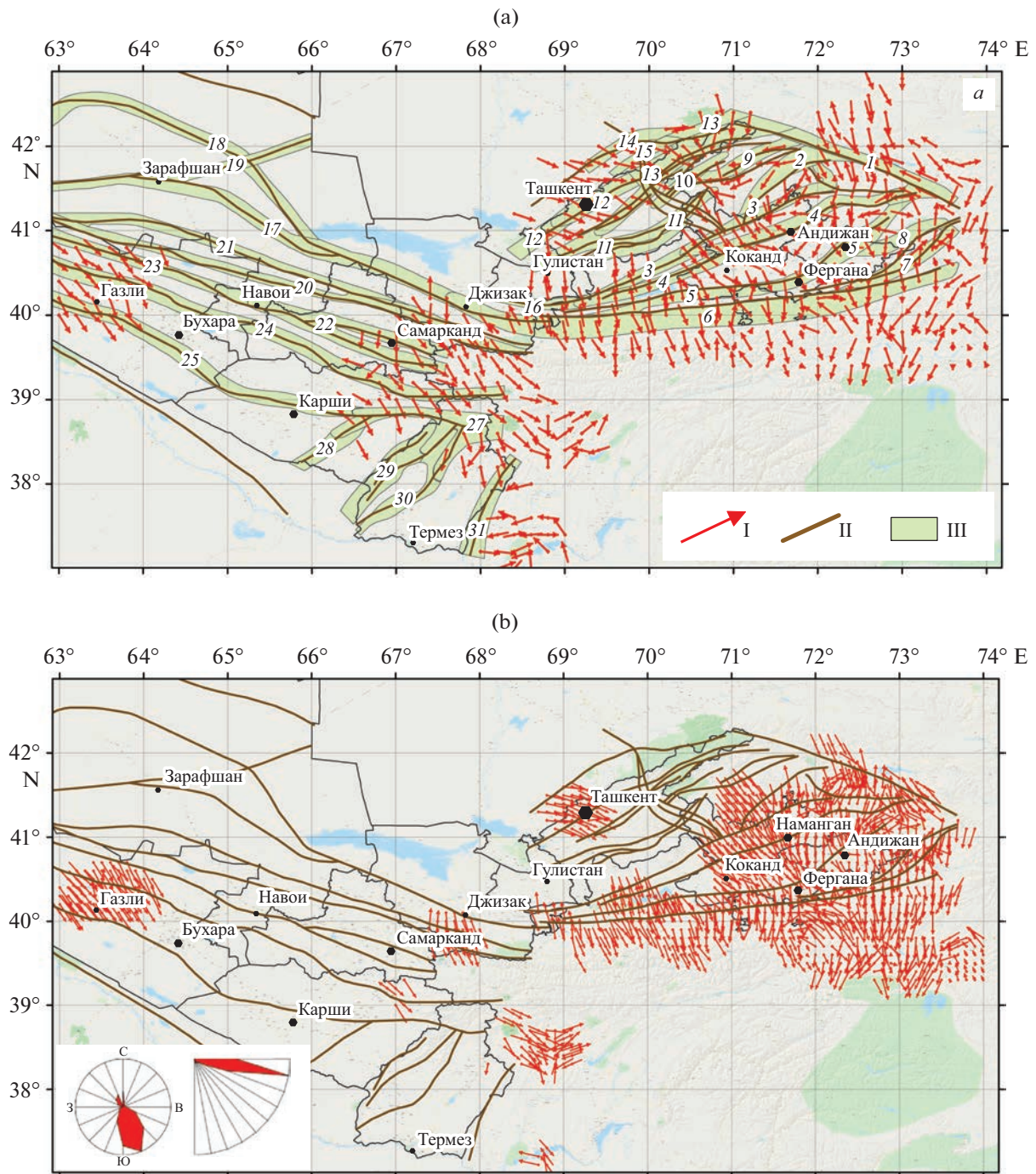


Fig. 9. Projections on horizontal plane of axis of algebraically minimal principal stresses (maximum compression) σ_3 with different reconstruction variants. (a) Over entire range of earthquake magnitudes with minimum size of uniform sampling $N \geq 5$ and maximum averaging radius $R \leq 60$ km; (b) for earthquakes with $M \leq 4.5$ with minimum uniform sampling size $N \geq 6$ and maximum radius $R \leq 30$ km; (c) earthquake with $M \geq 5$ with minimum uniform sampling size $N \geq 6$ and maximum radius $R \leq 30$ km of circular domain from which required number of events for single domain were selected. I, axis of minimum principal stress (maximum compression); II, active faults; III, seismogenic zones: 1, Talas-Fergana; 2, Chatkalo-Atoynak; 3, North Fergana; 4, Namangan; 5, Andijan; 6, South Fergana; 7, Kurshabskaya; 8, Taldyssuyskaya; 9, Chatkal; 10, Sandalash; 11, Angren; 12, Pskem-Tashkent; 13, Nurekatinskaya; 14, Langar; 15, Ugam-Karzhantau; 16, Mogoltau-Pistalitau; 17, Besapano-Severo-Nuratinskaya; 18, Bukuntauskaya; 19, Severo-Tamdynskaya; 20, North-Kuldzhuktau-Turkestan; 21, South Auminzatau-Aktau; 22, Zarafshan; 23, Predkizylkumskaya; 24, South Tien Shan; 25, Bukhara; 26, Sultanuzhdag; 27, Gissar-Kokshaalskaya; 28, Kyzildarya-Langarsky; 29, Baysun-Kugitang; 30, Surkhantau-Sherabad-Kelif; 31, Babatag-Keikitauskaya.

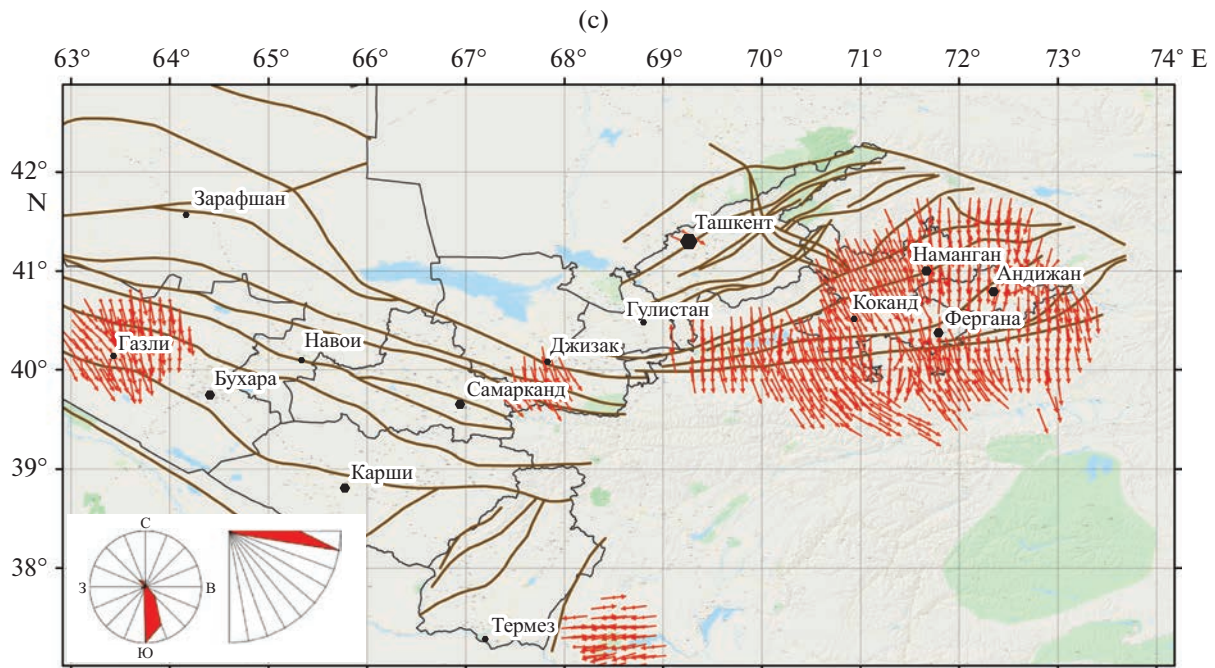


Fig. 9. (Contd.)

employing mechanisms with different magnitude levels. For the Gazli focal zone, the azimuth of the σ_3 axis changes, as a result of stress reconstruction for strong earthquakes, from southeast (obtained for weak to moderate earthquakes) to south at about the same dip angle, and the dip of the σ_1 axis when considering only strong earthquakes becomes almost subvertical. The same can be said about the dip angle of the σ_1 axis for the section between the cities of Jizzakh and Samarqand, related to the Nurata and Zirabulak-Ziaetda ranges. For the Pristashkent region and for the Fergana intermontane depression, there is good agreement between the strike azimuths and dip angles of the σ_3 and σ_1 axes at this level of detail when considering earthquakes with different energy levels. The direction of the principal axis of maximum compressive stress σ_3 for the territory of the Pristashkent region is sublatitudinal, and the axis of minimal compression σ_1 is oriented south-southwest. The dip of both the σ_1 and σ_3 axes for most domains is quite gentle.

Analysis of the distribution of the Lode–Nadai coefficient calculated over the entire set of earthquakes (Fig. 11a) with a large averaging radius indicates that the predominant number of domains is characterized by a state close to simple shear ($-0.2 < \mu_\sigma < 0.2$). Domains with a stress state close to uniaxial compression ($\mu_\sigma \geq 0.6$) or uniaxial tension ($\mu_\sigma \leq -0.6$) are distributed throughout the study area in a somewhat mosaic pattern.

At the detailed level of reconstruction ($R \leq 30$ km), when considering the EFM with $M \leq 4.5$, the share of domains with a stress state close to simple shear decreases somewhat (Figs. 11b, 11c), and domains in which the form of the stress state is close to uniaxial compression or uniaxial tension acquire the features of an associated set. Areas with $\mu_\sigma \geq 0.2$ are located in the east and west of the Gazli focal zone, in the central part of the South Fergana seismically active zone, and in the northern part of the Babatag–Keikitau structure. Two regions with a stress state close to uniaxial tension ($\mu_\sigma \leq -0.2$) are situated within the Fergana intermontane depression north of the cities of Andijan and Namangan, and one within the Alai valley beyond the Alai ridge. Several domains within the Pristashkent region are also characterized by moderate negative Lode–Nadai coefficients.

Based on the results of the stress reconstruction obtained using the EFM with $M \geq 5$ from the consolidated EFM catalog, domains with a stress state close to uniaxial compression are located in the northern part of the Gazli focal zone, in the junction zone of the South Fergana and North Fergana seismically active zones, as well as in the areas of the Alai and Turkestan ridges. Domains with a stress state close to uniaxial tension are observed only within two sections of the Fergana intermontane depression: between the North Fergana fault and the South Fergana flexure–fracture zone south of Kokand and north of Andijan within the

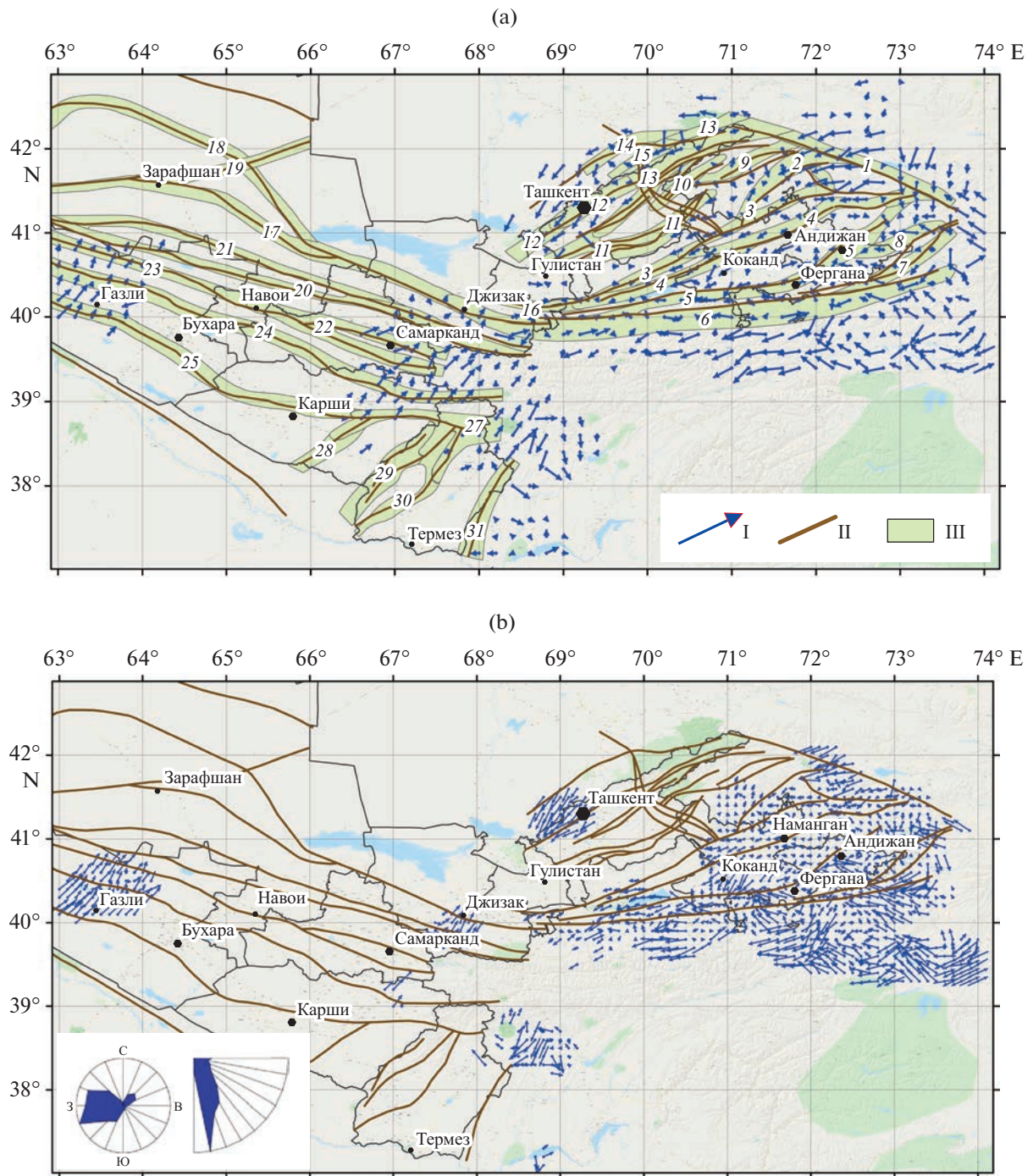


Fig. 10. Projections on horizontal plane of axis of algebraically minimum compression σ_1 (main deviatoric tension) σ_3 with different reconstruction variants. (a) Over entire range of earthquake magnitudes with minimum size of uniform sampling $N \geq 5$ and maximum averaging radius $R \leq 60$ km; (b) for earthquakes with $M \leq 4.5$ with minimum uniform sampling size $N \geq 6$ and maximum radius $R \leq 30$ km; (c) earthquake with $M \geq 5$ with minimum uniform sampling size $N \geq 6$ and maximum radius $R \leq 30$ km of circular domain from which the required number of events for single domain were selected; I, axis of minimum principal stress (maximum compression); II, active faults; III, seismogenic zones (see names in caption to Fig. 9).

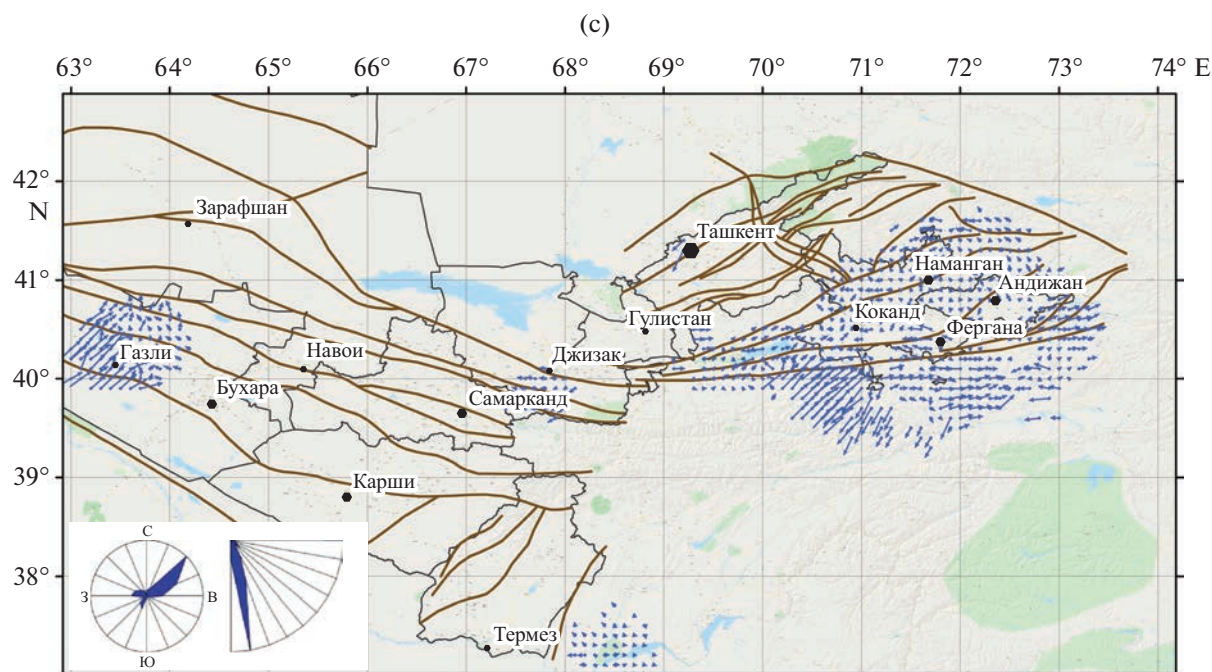


Fig. 10. (Contd.)

Andijan seismogenic zone. The share of regions with a stress state close to the simple shear becomes even smaller than as a result of the previous reconstruction based on the EFM for weak and moderate earthquakes.

Zoning of the Territory by Geodynamic Types of Stress State

Based on the results of the reconstruction for the entire set of EFM from the EFM catalog with a minimum number of events in a single uniform sampling of $N \geq 5$ and maximum radius of $R \leq 60$ km of the circular domain from which the required number of events for a single domain were selected (Fig. 12a), the prevailing geodynamic type of stress state for the entire study area is a horizontal compression regime. Domains characterized by a horizontal shear regime are located in the central part of the Talas-Fergana seismically active zone and in southern Uzbekistan in the northern part of the Babatag-Keikitau seismogenic zone. Small sectors characterized by a horizontal shear regime are also located in the northeastern part of the seismically active structures of the Pristashkent region and on separate segments of the South Tien Shan seismically active zone outside eastern Uzbekistan. The largest number of domains in the horizontal tensile regime are located behind the Turkestan ridge and within the Alai Valley. In these areas, the axis of minimum compression σ_1 is subhorizontal and oriented in the direction of the strike of the South Tien Shan seismically active zone, and the axis

of maximum compression σ_3 has a direction across structures and is vertical.

According to the results of a more detailed reconstruction based on EFM of weak and moderate earthquakes (Fig. 12b), the location of areas characterized by different geodynamic types of stress state has not changed significantly. The horizontal shear domain in the Gazli focal zone increased insignificantly, and a small number of domains with this geodynamic type of stress state appeared west of Tashkent.

In the part of the territory where it was possible to carry out a detailed reconstruction of the focal mechanisms of strong earthquakes, only two types of stress state are observed: the horizontal compression and horizontal shear regimes (Fig. 12c). The latter type is characteristic of the western part of the Gazli focal zone and the zone geographically located between the Turkestan and Alai ridges.

In our opinion, the differences in the same domains of parameters of the stress state of the crust at the detailed level of reconstruction ($R_{\max} \leq 30$ km) for hierarchically different magnitude ranges of the considered earthquakes ($M \leq 4.5$ and $M \geq 5$) occur because the magnitude hierarchy of earthquakes governs the different depths of tectonic processes occurring in the crust. Figure 13 shows the depth distribution of earthquakes in Uzbekistan.

With an increase in the energy class of an earthquake, the average depth of its hypocenter increases. The energy class $K = 12.5$ ($M = 4.5$) corresponds to an average depth $H = 15$ km; therefore, reconstruction of

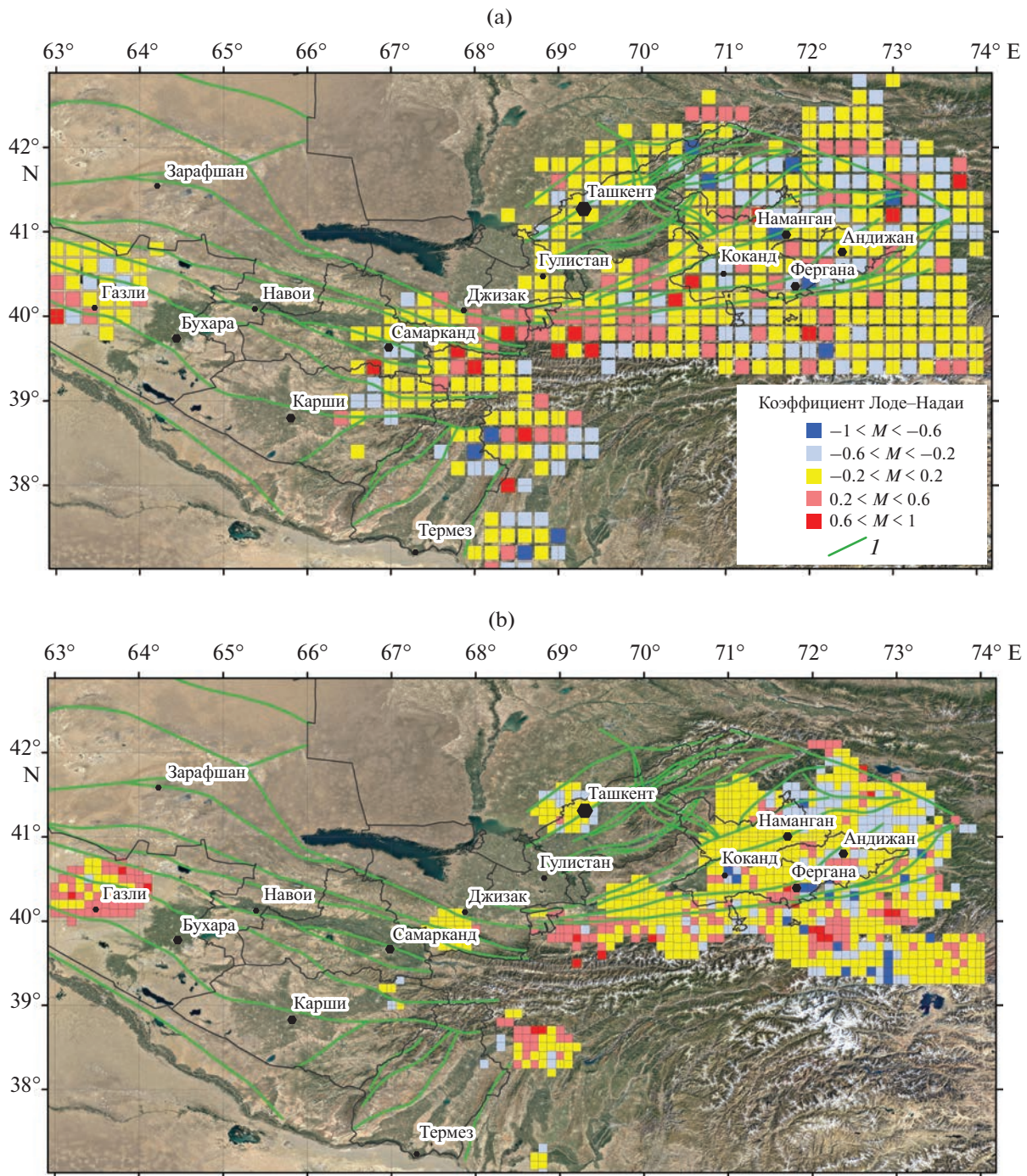


Fig. 11. Area distribution of Lode–Nadai coefficient with different reconstruction variants. (a) Over entire range of earthquake magnitudes with minimum size of uniform sampling $N \geq 5$ and maximum averaging radius $R \leq 60$ km; (b) for earthquakes with $M \leq 4.5$ with minimum uniform sampling size $N \geq 6$ and maximum radius $R \leq 30$ km; (c) earthquake with $M \geq 5$ with minimum uniform sampling size $N \geq 6$ and maximum radius $R \leq 30$ km of circular domain from which required number of events for single domain were selected; I , active faults.

earthquakes with $M \leq 4.5$ reflects the stress state of the upper (up to 15 km) layer of the crust, while reconstruction of earthquakes with $M \geq 5$ characterizes the stress state of a deeper layer ($H \geq 15$ km).

Relative Maximum Shear Stresses and Effective Uniform Pressure

One result of the second stage of stress reconstruction using CAM is the determination of the relative

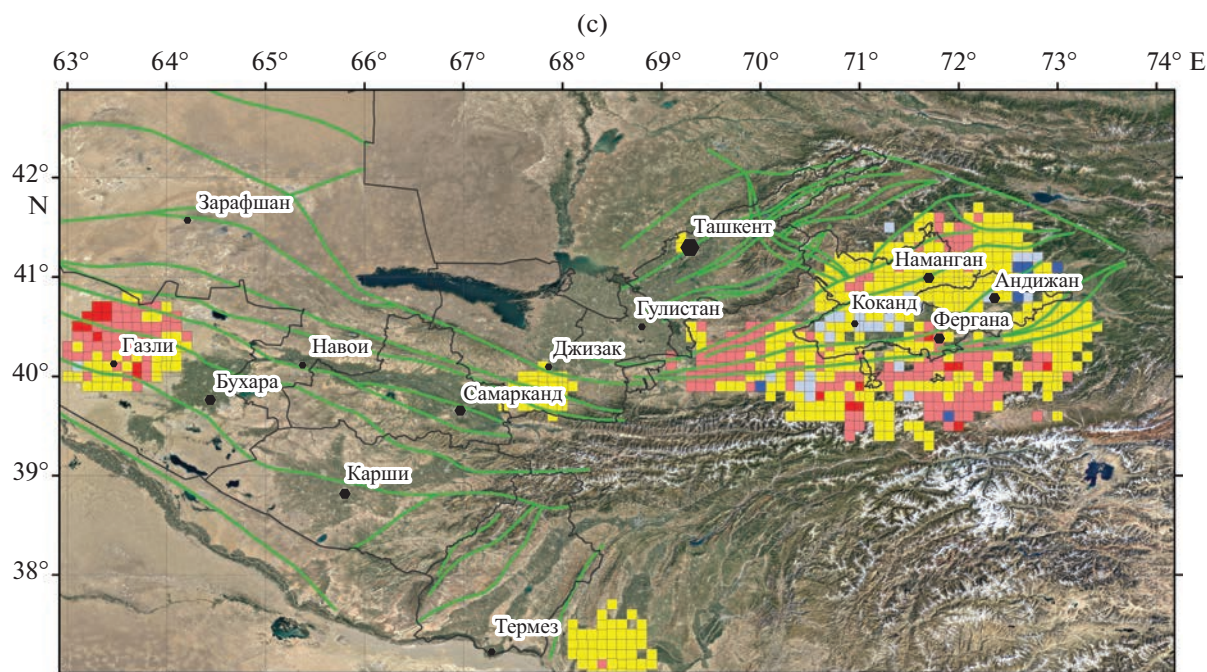


Fig. 11. (Contd.)

maximum tangential stresses and effective uniform pressure (the difference between the pressure in the rocks and the fluid pressure of the fracture-pore space: $p^* = p - p_{fl}$, where $p = -(\sigma_1 + \sigma_2 + \sigma_3)/3$). With this method, it is assumed that in domains characterized by high seismic activity, rock massifs are in a stress state close to the limiting state. From the Coulomb–Mohr relations, this governs the directly proportional relationship between the effective normal σ_1^* and tangential τ_n stresses on the brittle fracture plane (Rebetsky, 1997) and therefore between their relative values p^*/τ_f and τ/τ_f , obtained by normalizing the p^* and τ values to the cohesion strength of rock massifs τ_f (assuming that the latter does not vary much within the study area).

Figure 14 shows the area distribution of relative effective pressure p^*/τ_f for different variants of the reconstruction (in view of the above, the behavior of τ/τ_f is similar to changes in p^*/τ_f and therefore is not given below).

For the first two reconstruction variants (over the entire range of earthquake magnitudes with the minimum size of uniform sampling $N \geq 5$ and maximum radius $R \leq 60$ km and earthquakes with $M \leq 4.5$ with a minimum uniform sampling size $N \geq 6$ and maximum radius $R \leq 30$ km), the area distribution of increased, moderate, and decreased parameter values p^*/τ_f have a quite mosaic pattern (see Figs. 14a, 14b). According to the results of reconstruction using the EFM of strong earthquakes, it can be seen that domains with different relative values of the effective pressure p^*/τ_f

are much better structured and alternate among themselves on the territory of eastern Uzbekistan within the South Fergana and North Fergana faults and flexure-fracture zones of the same name. In the western part of Uzbekistan, lower effective pressures p^*/τ_f are characteristic of the Gazli focal zone.

In (Rebetsky 2007; Rebetsky and Tatevossian, 2013; Rebetsky et al., 2016), it was noted that strong earthquakes usually occur in areas with low effective uniform pressures and maximum shear stresses. This is because in such regions, the values of friction forces on ruptures are reduced, and this creates favorable conditions for large-scale faulting. In order to verify this position in the studied region, we mapped the normalized values of the effective pressure to the epicenters of earthquakes with magnitudes $M \geq 5.5$ that had occurred in Uzbekistan since historical times. In general, based on the results of the reconstruction carried out with a high level of detail (see Figs 14b, 14c), it can be seen that the distribution of such earthquakes does not contradict the conclusions of these papers established from studying other seismically active regions. Therefore, the rather long sectors of lower values of normalized effective pressures p^*/τ_f within high-potential zones in eastern Uzbekistan are noteworthy (see Fig. 14c), obtained from the results of reconstruction involving the focal mechanisms of strong earthquakes. These values were obtained from the reconstruction using the focal mechanisms of strong earthquakes, which, as noted above, characterizes the stress state of a lower seismically active layer, where, in fact, strong earthquakes occur. For a more

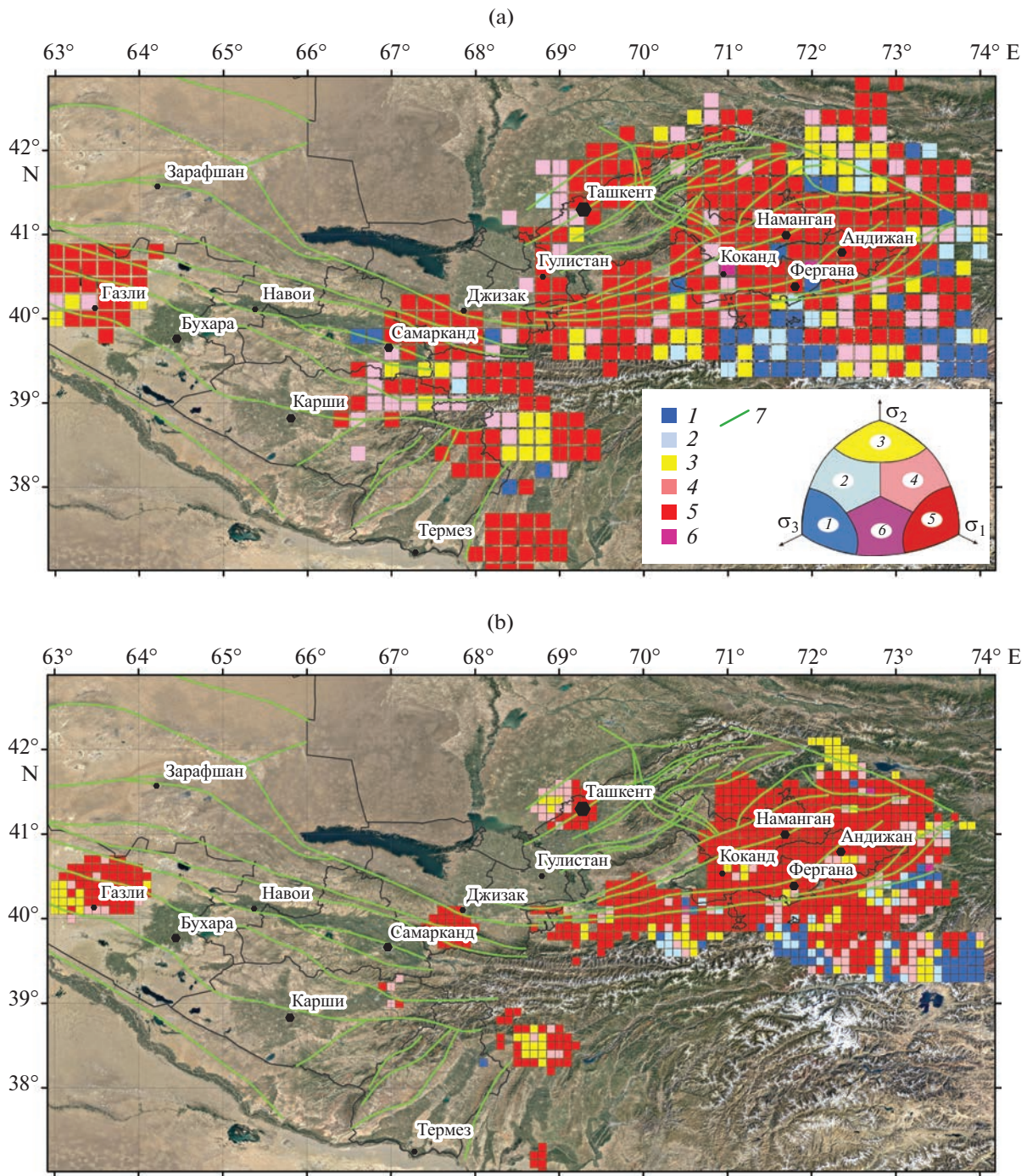


Fig. 12. Zoning of territory by geodynamic types of stress state with different reconstruction variants and, over the entire range of earthquake magnitudes with a minimum size of a uniform sampling $N \geq 5$ and maximum radius $R \leq 60$ km; *b*, for earthquakes from $M \leq 4.5$ with a minimum uniform sampling size $N \geq 6$ and maximum radius $R \leq 30$ km; *in*, earthquake with $M \geq 5$ with a minimum uniform sampling size $N \geq 6$ and maximum radius $R \leq 30$ km of a circular region from which the required number of events for a single domain was selected; 1-6, types of stress state: 1, horizontal tension; 2, horizontal tensile shear; 3, horizontal shear; 4, horizontal compressive shear; 5, horizontal compression; 6, shear in vertical plane; 7, active faults.

specific tectonophysical zoning of hazardous sections of these faults, special studies of Coulomb stresses on

their surfaces are required, which requires data on the dip angles of faults (Rebetsky and Kuzikov, 2016).

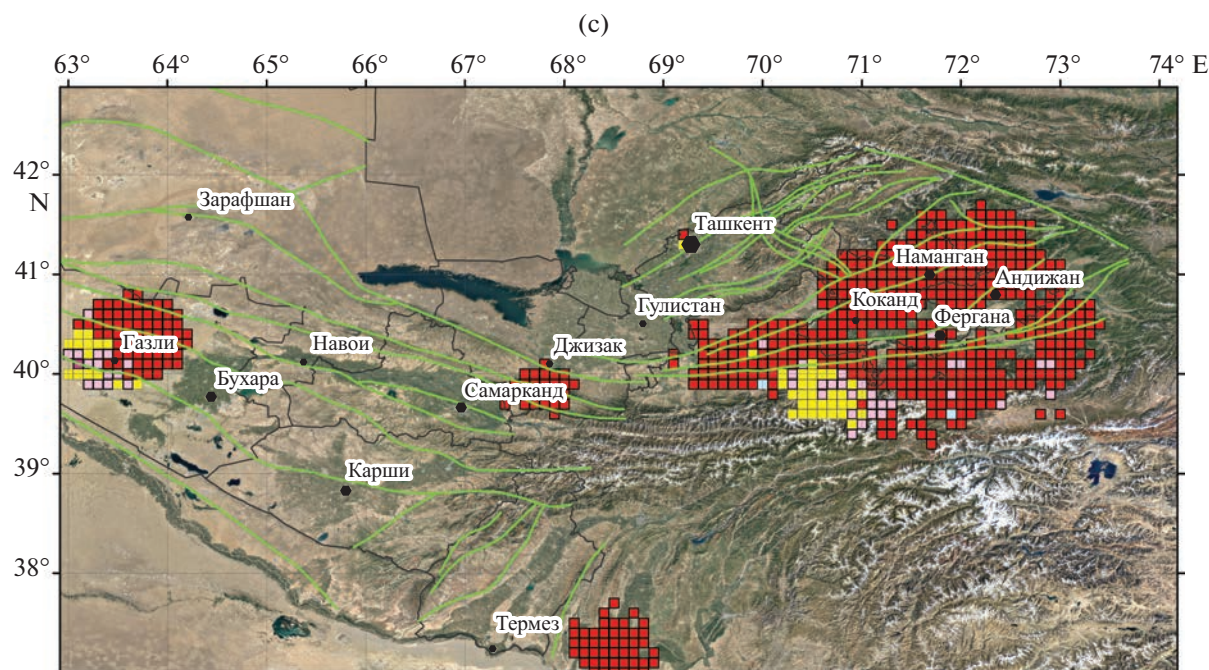


Fig. 12. (Contd.)

CONCLUSIONS

Based on the consolidated EFM catalog compiled by different authors, cataclastic analysis methods (CAM) for discontinuous displacements are used to study the current stress state of the crust in Uzbekistan. Two stages of the reconstruction of the stress field by the CAM method were implemented at different levels of area detail of the averaging parameters and with different magnitude hierarchies of the considered earthquakes. The azimuths and dip angles of the axes of principal stresses, the Lode–Nadai coefficients, the geodynamic types of stress state normalized to the cohesion strength of rock massifs, the maximum tangential stresses, and effective uniform pressure are determined. Corresponding maps of the area distribution of the indicated parameters were constructed.

When the averaging window is varied from 10 to 60 km and the minimum number of focal mechanisms falling into the uniform sampling of seismic events is 5, the stress state parameters of rock massifs were obtained for almost the entire seismically active part of the territory of Uzbekistan. For individual domains of the study area at two hierarchical levels (for weak and moderate earthquakes with $M \leq 4.5$ and for strong earthquakes with $M \geq 5$), reconstruction was possible with a higher level of detail for an averaging scale within a single domain from 15 to 30 km and a minimum number of earthquakes falling into a uniform sampling of 6.

Analysis of the spatial position of the axes of principal stresses showed that the dip angle of the axis of minimal compression varies greatly for different sec-

tors of the studied territory, varying from vertical in southern Uzbekistan to almost horizontal in the Alai Valley. Variations in the dip angle of the axis of main compressive stress are significantly less. For most of the territory, this axis is subhorizontal, and its azimuth is almost perpendicular to the direction of tectonic structures. This feature is violated for the southeastern part of the Talas–Fergana fault, where the directions of the fault and axis of maximum compression almost coincide.

With a large averaging radius, the predominant number of domains is characterized by a state close to simple shear (the Lode–Nadai coefficient is close to zero), and domains with a stressed state close to uniaxial compression ($\mu_\sigma \geq 0.6$) or uniaxial tension ($\mu_\sigma \leq -0.6$) are distributed in a rather mosaic pattern over the study area. At the detailed level of reconstruction ($R \leq 30$ km) when the focal mechanisms of earthquakes with $M \leq 4.5$, the fraction of regions with a stress state close to a pure shear decreases, and regions in which the form of a stress state is close to uniaxial compression or uniaxial tension acquire the features of an associated set. The former are located in the east and west of the Gazli focal zone, in the central part of the South Fergana seismically active zone, and in the northern part of the Babatag–Keikitau structure; the latter are located within the Fergana intermontane basin and the Alai Valley. According to the results of stress reconstruction obtained using the EFMs with $M \geq 5$, the fraction of domains with a stress state close to uniaxial compression is almost commensurate with that of domains where the stress state is close to simple

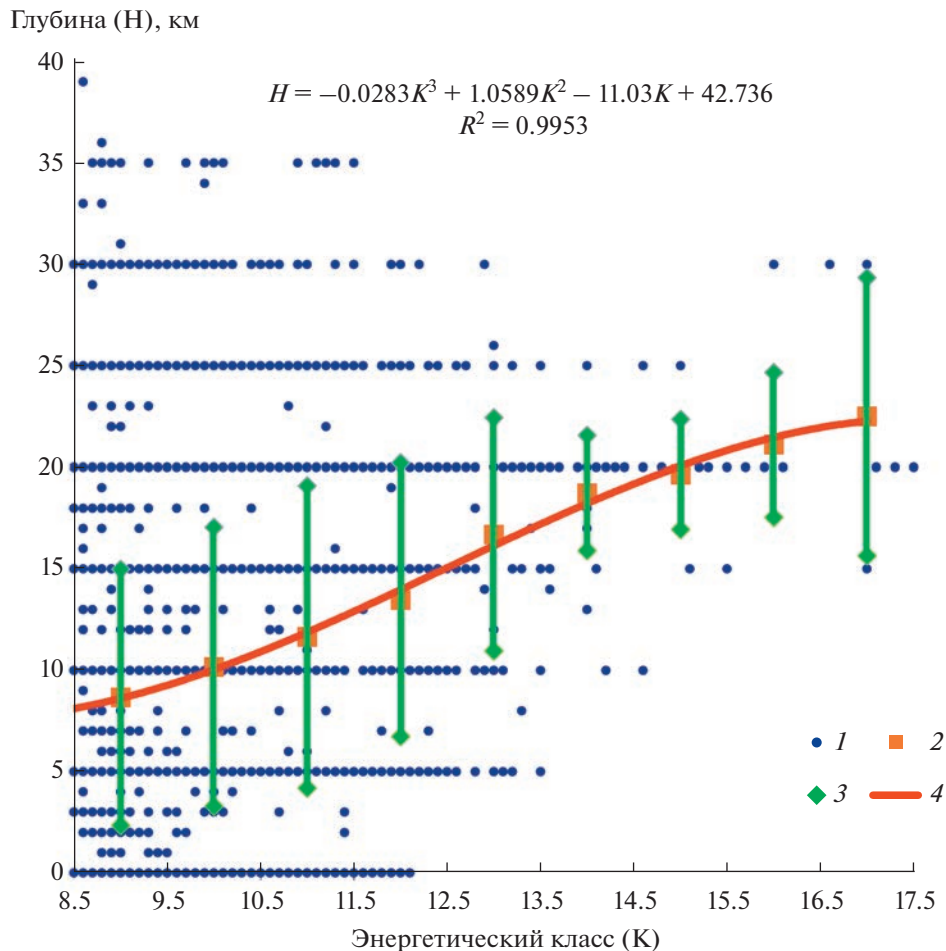


Fig. 13. Depth distribution of earthquakes of various energy classes in territory of Uzbekistan. (1) depth distribution of earthquakes; (2) average depth values for each energy class; (3) standard deviations; (4) polynomial approximation of dependence $H = f(K)$.

shear, and regions with a stress state close to uniaxial tension almost completely disappear.

With the same large averaging radius, the prevailing type of stress state for the entire study area is a horizontal compression regime. Domains characterized by a horizontal shear regime are located in the central part of the Talas-Fergana seismically active zone and in southern Uzbekistan. The largest number of domains in the horizontal tensile regime are located behind the Turkestan ridge and within the Alai Valley.

According to the results of a more detailed reconstruction based on the focal mechanisms of weak and moderate earthquakes, the location of domains characterized by different types of geodynamic regimes did not change significantly. In the part of the territory where detailed reconstruction of the focal mechanisms of strong earthquakes was possible, only two types of stress state are observed: horizontal compression and horizontal shear regimes. The latter type is characteristic of the western part of the Gazli focal

zone and the domain geographically located between the Turkestan and Alai ranges.

A possible reason for the difference in the stress state parameters in the same domains during reconstructions based on EFM's with different magnitude ranges ($M \leq 4.5$ and $M \geq 5$) is the fact that the magnitude hierarchy of earthquakes governs the different depths of tectonic processes occurring in the 'crust. Reconstruction of earthquakes with $M \leq 4.5$ reflects the stress state of the upper (up to 15 km) layer of the crust, and reconstruction of earthquakes with $M \geq 5$ characterizes the stress state of a deeper layer ($H \geq 15$ km).

Segments of active faults with a decreased effective pressure level were identified in the territory of eastern Uzbekistan. Taking into account the relationship between sectors with such properties and location of focal zones of strong earthquakes established earlier for other seismically active regions, these segments of active crustal faults are considered zones of potentially increased seismic hazard. For them, it is necessary to

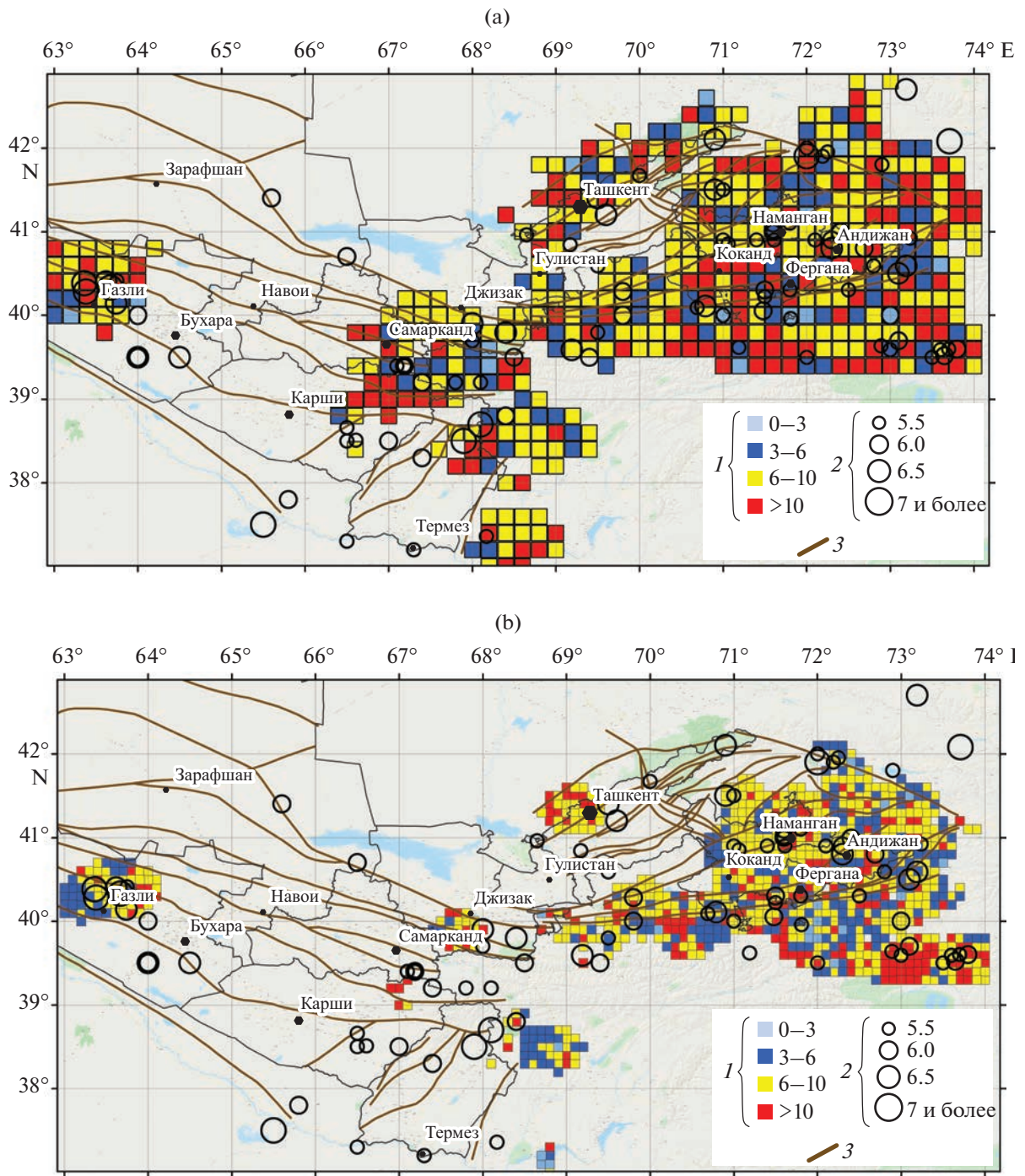


Fig. 14. Area distribution of effective pressure normalized to cohesion strength (p^*/τ_f) for different reconstruction variants. (a) Over the entire range of earthquake magnitudes with minimum size of uniform sampling $N \geq 5$ and maximum radius $R \leq 60$ km; (b) for earthquakes with $M \leq 4.5$ with minimum uniform sampling size $N \geq 6$ and maximum radius $R \leq 30$ km; (c) earthquake with $M \geq 5$ with minimum uniform sampling size $N \geq 6$ and maximum radius $R \leq 30$ km of circular domain from which required number of events for single domain were selected; 1, p^*/τ_f -values; 2, epicenters of earthquakes with $M \geq 5.5$; 3, active faults.



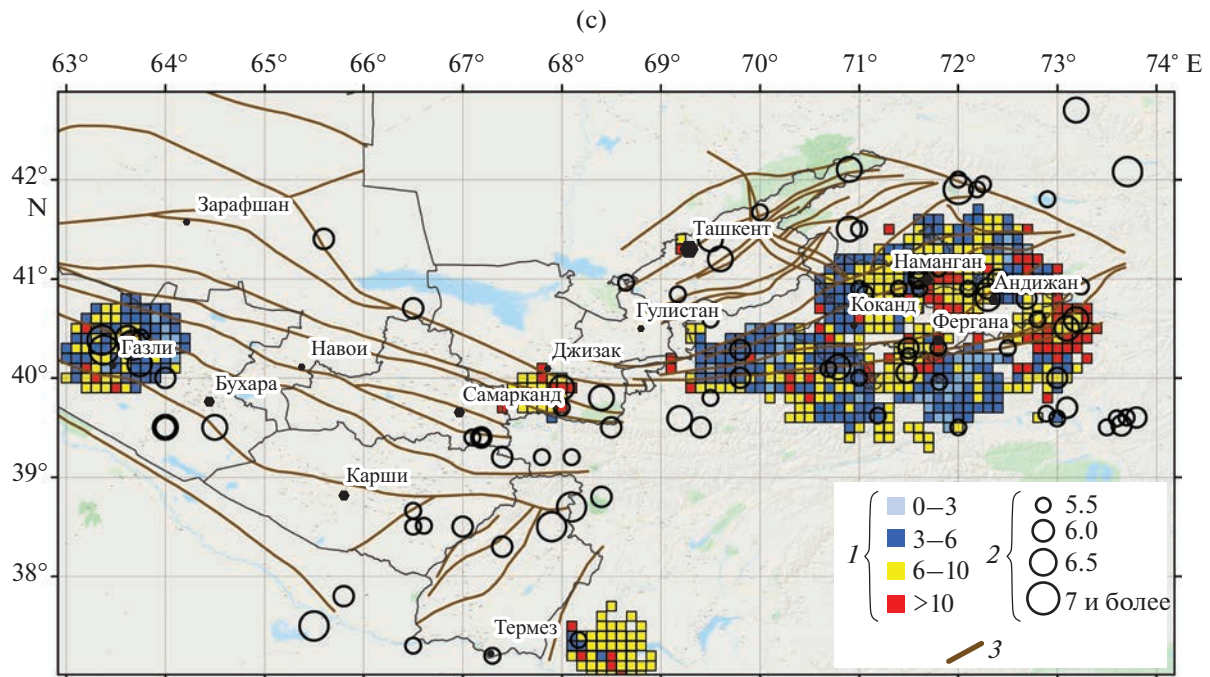


Fig. 14. (Contd.)

continue research using tectonophysical methods for zoning hazardous faults.

FUNDING

The study was carried out within the state task of IPE RAS and supported by state basic research grant FA-F8-007 of the Ministry of Innovative Development of the Republic of Uzbekistan.

ACKNOWLEDGMENTS

The authors thank the reviewers, especially one of them, for a thorough analysis of the article and comments.

CONFLICT OF INTEREST

The authors declare no conflict of interest.

REFERENCES

- Artikov, T.U., Ibragimov, R.S., Ibragimova, T.L., and Mirzaev, M.A., Synoptical long-term forecast of possible locations of seismic activations in the territory of Uzbekistan, *Georisk*, 2017, no. 2, pp. 20–28.
- Artikov, T.U., Ibragimov, R.S., Ibragimova, T.L., and Mirzaev, M.A., Identification of expected seismic activity areas by forecasting complex seismic-mode parameters in Uzbekistan, *Geod. Geodyn.*, 2018, vol. 9, no. 2, pp. 121–130.

- Artikov, T.U., Ibragimov, R.S., Ibragimova, T.L., and Mirzaev, M.A., Complex of general seismic zoning maps OSR-2017 of Uzbekistan, *Geod. Geodyn.*, 2020, vol. 11, no. 4, pp. 273–292.

<https://doi.org/10.1016/j.geog.2020.03.004>

- Atabekov, I.U., Earth Core's stresses variation in Central Asian earthquakes region, *Geod. Geodyn.*, 2020, vol. 11, no. 4, pp. 293–299.

<https://doi.org/10.1016/j.geog.2019.12.005>

- Bezrodnyi, E.M. and Tuichiev, Kh.A., *Mekhanizmy ocha-gov sil'nykh zemletryasenii Uzbekistana* (Focal Mechanisms of Strong Earthquakes of Uzbekistan), Tashkent: Fan, 1987.

Global CMT. <http://www.globalcmt.org>. Accessed April 17, 2014.

- Gushchenko, O.I., Seismotectonic stress monitoring of the lithosphere: Structural kinematic principle and basic features of the algorithm), *Dokl. Earth Sci.*, 1996, vol. 346, no. 1, pp. 144–147.

- Gushchenko, O.I. and Sim, L.A., The field of modern megaregional stresses in seismoactive regions of southern Eurasia, *Izv. Akad. Nauk SSSR. Geol. Razved.*, 1977, no. 12.

- Gushchenko, O.I., Stepanov, V.V., and Sim, L.A., Directions of modern megaregional stresses in seismoactive regions of southern Eurasia, *Dokl. Akad. Nauk SSSR. Ser. Geofiz.*, 1977, vol. 234, no. 3, pp. 556–559.

- Gzovskii, M.V., *Osnovy tektonofiziki* (Fundamentals of Tectonophysics), Moscow: Nauka, 1975.

- Ibragimov, R.N., Nurmatov, U.O., and Ibragimov, O.R., Seismotectonic method of seismic hazard assessment and problems of seismic zoning, in *Seismicheskoe raionirovanie i prognoz zemletryasenii v Uzbekistane* (Seismic Zoning and

- Earthquake Prediction in Uzbekistan), Tashkent: Gidroiingeo, 2002, pp. 59–74.
- Khamidov, L.A., Calculation of stresses and strains in source zones of strong earthquakes, *Dokl. Akad. Nauk Resp. Uzb.*, 2004, no. 6, pp. 33–37.
- Kuznetsova, K.I., Mikhaylova, R.S., Bagmanova, N.Kh., Muraliev, A.M., Matasova, L.M., Seyduzova, S.S., and Soboleva, O.V., A set of seismic parameters and recent tectonic movements in the Alpine tectonic belt. Part I. 1. Method of study. 2. Tien Shan and Pamirs, *Phys. Solid Earth*, 1995, vol. 31, no. 10, pp. 844–857.
- Mukambaev, A.S. and Mikhailova, N.N., Solution of the problem of magnitude inhomogeneity in the framework of seismic sounding works in the Republic of Kazakhstan, *Vestn. Nats. Yad. Tsentra Resp. Kaz.*, 2014, no. 4, pp. 86–92.
- Nikolaev, P.N., *Metodika termodinamicheskogo analiza* (Technique of Thermodynamic Analysis), Moscow: Nedra, 1992.
- Rautian, T.G., Energy of earthquakes, in *Metody detal'nogo izucheniya seismichnosti* (Methods of Detailed Studies of Seismicity), vol. 176 of *Tr. GeoFIAN*, Moscow: Akad. Nauk SSSR, 1960, ch. 3, pp. 75–114.
- Rautian, T.G., Khalturin, V.I., Fujita, K., Mackey, K.G., and Kendall, A.D., Origins and methodology of the Russian energy K-class system and its relationship to magnitude scales, *Seismol. Res. Lett.*, 2007, vol. 78, no. 6, pp. 579–590.
- Rebetskii, Yu.L., Stressed state corresponding to the formation of large-scale brittle failure of rocks, *Dokl. Earth Sci.*, 2007, vol. 417, no. 8, pp. 1216–1220.
- Rebetsky, Yu.L., Reconstruction of tectonic stresses and seismotectonic strains: Methodical fundamentals, current stress field of Southeastern Asia and Oceania, *Dokl. Earth Sci.*, 1997, vol. 354, no. 4, pp. 560–563.
- Rebetsky, Yu.L., The current state of crustal stresses in the Caucasus according to the unified catalog of earthquake focal mechanisms, *Geodin. Tektonofiz.*, 2020, vol. 11, no. 1, pp. 17–29.
<https://doi.org/10.5800/GT-2020-11-1-0459>
- Rebetsky, Yu.L. and Kuzikov, S.I., Active faults of the northern Tien Shan: Tectonophysical zoning of seismic risk, *Russ. Geol. Geophys.*, 2016, vol. 57, no. 6, pp. 967–983.
<https://doi.org/10.1016/j.rgg.2016.05.004>
- Rebetsky, Yu.L. and Tatevossian, R.E., Rupture propagation in strong earthquake sources and tectonic stress field, *Bull. Soc. Geol. Fr.*, 2013, vol. 184, nos. 4–5, pp. 335–346.
- Rebetsky, Yu.L., Sycheva, N.A., Sychev, V.N., Kuzikov, S.I., and Marinin, A.V., The stress state of the Northern Tien Shan crust based on the KNET seismic network data, *Russ. Geol. Geophys.*, 2016, vol. 57, no. 3, pp. 387–408.
- Riznichenko, Yu.V., *Izbrannye trudy. Problemy seismologii* (Selected Papers on Problems of Seismology), Moscow: Nauka, 1985.
- Riznichenko, Yu.V., Soboleva, O.V., Kuchai, O.A., Mikhailova, R., and Vasil'eva, O.N., Seismotectonic deformation of the Earth's crust in southern Central Asia, *Izv. Akad. Nauk SSSR. Fiz. Zemli*, 1982, no. 10, pp. 90–104.
- Shirokova, E.I., Detailed study of stresses and ruptures in sources of Central Asian earthquakes, *Izv. Akad. Nauk SSSR. Fiz. Zemli*, 1974, no. 11, pp. 23–36.
- Sobolev, G.A. and Ponomarev, A.V., *Fizika zemletryaseni i predvestniki* (Earthquake Physics and Precursors), Moscow: Nauka, 2003.
- Trifonov, V.G., Soboleva, O.V., Trifonov, R.V., and Vostrikov, G.A., *Sovremennaya geodinamika Al'piisko-Gimalaiskogo kollizionnogo poyasa* (Modern Geodynamics of the Alpine–Himalayan Collisional Belt), Moscow: GEOS, 2002.
- Ulomov, V.I., *Dinamika zemnoi kory Srednei Azii i prognoz zemletryaseni* (Dynamics of the Earth's Crust of Central Asia and Earthquake Forecast), Tashkent: Fan, 1974.
- Umurzakov, R.A., Structural and seismic indications of the elements of recent and present-day stress fields in several epicentral regions of western Tien Shan, *Izv., Phys. Solid Earth*, 2010, vol. 46, no. 5, pp. 379–386.
- Yunga, S.L., *Metody i rezul'taty izucheniya seismotektonicheskikh deformatsii* (Methods and Results of Studying Seismotectonic Deformations), Moscow: Nauka, 1990.
- Zemletryaseniya Srednei Azii i Kazakhstana* (Earthquakes of Central Asia and Kazakhstan), Dushanbe: Donish, 1979–1988.

SPELL: 1. figs